European Journal of Medicinal Chemistry 81 (2014) 192–203

Contents lists available at ScienceDirect

European Journal of Medicinal Chemistry

journal homepage: http://www.elsevier.com/locate/ejmech

Original article

Design, synthesis and molecular docking studies of novel *N*-benzenesulfonyl-1,2,3,4-tetrahydroisoquinoline-based triazoles with potential anticancer activity

Ratchanok Pingaew [a,*], Prasit Mandi [b,c], Chanin Nantasenamat [b,c], Supaluk Prachayasittikul [b], Somsak Ruchirawat [d,e,f], Virapong Prachayasittikul [c]

[a] Department of Chemistry, Faculty of Science, Srinakharinwirot University, Bangkok 10110, Thailand
[b] Center of Data Mining and Biomedical Informatics, Faculty of Medical Technology, Mahidol University, Bangkok 10700, Thailand
[c] Department of Clinical Microbiology and Applied Technology, Faculty of Medical Technology, Mahidol University, Bangkok 10700, Thailand
[d] Laboratory of Medicinal Chemistry, Chulabhorn Research Institute, Bangkok 10210, Thailand
[e] Program in Chemical Biology, Chulabhorn Graduate Institute, Bangkok 10210, Thailand
[f] Center of Excellence on Environmental Health and Toxicology, Commission on Higher, Education (CHE), Ministry of Education, Thailand

ARTICLE INFO

Article history:
Received 23 December 2013
Received in revised form
1 May 2014
Accepted 4 May 2014
Available online 6 May 2014

Keywords:
Isoquinoline
Triazole
Pictet–Spengler reaction
Antiproliferative activity
Molecular docking
AKR1C3

ABSTRACT

A novel series of *N*-benzenesulfonyl-1,2,3,4-tetrahydroisoquinolines (**14**–**33**) containing triazole moiety were designed and synthesized through rational cycloadditions using the modified Pictet–Spengler reaction and the Click chemistry. Antiproliferative activity against four cancer cell lines (e.g., HuCCA-1, HepG2, A549 and MOLT-3) revealed that many substituted triazole analogs of benzoates (**20**, **29**) and benzaldehydes (**30**, **32**) exhibited anticancer activity against all of the tested cancer cell lines in which the ester analog **20** was shown to be the most potent compound against HuCCA-1 (IC_{50} = 0.63 μM) and A549 (IC_{50} = 0.57 μM) cell lines. Triazoles bearing phenyl (**15**, **24**), tolyl (**26**, **27**), acetophenone (**19**), benzoate (**20**, **29**), benzaldehyde (**21**, **30**) and naphthalenyl (**25**) substituents showed stronger anticancer activity against HepG2 cells than that of the etoposide. Interestingly, the *p*-tolyl analog (**27**) displayed the most potent inhibitory activity (IC_{50} = 0.56 μM) against HepG2 cells without affecting normal cells. Of the investigated tetrahydroisoquinoline-triazoles, the promising compounds **20** and **27** were selected for molecular docking against AKR1C3, which was identified to be a plausible target site.

1. Introduction

Isoquinoline alkaloid is a class of natural products that possess a broad spectrum of pharmacological actions, particularly, anticancer activity [1–3]. A variety of bioactive 1,2,3,4-tetrahydroisoquinolines (THIQs) have been reported. Generally, THIQs are synthesized by the Pictet–Spengler reaction involving the cyclization of iminium ions derived from the condensation of β-arylethylamines with aldehydes [4,5]. The modified Pictet–Spengler protocol was accomplished by increasing the electrophilicity of the iminium intermediates using *N*-sulfonylphenethylamines as starting materials to yield *N*-sulfonyl-1,2,3,4-tetrahydroisoquinoline products. Such *N*-sulfonyl-THIQs have been proven to be interesting scaffolds for medical applications [6,7]. 1,2,3,4-Tetrahydro-6,7-dimethoxy-2-[(4-methylphenyl)sulfonyl]-1-(2-hydroxyphenylisoquinoline) (**1**) and 1-acetyl-6,7-dimethoxy-*N*-4-methoxybenzenesulfonyl-1,2,3,4-tetrahydroisoquinoline thiosemicarbazone (**2**) exhibited cytotoxic activity reported by our group as shown in Fig. 1 [6,7]. Furthermore, *N*-sulfonyl-THIQ (**3**) and *N*-sulfonyl-THIQs with hydroxamate (**4**) and carboxylate (**5**) have been revealed to act as carbonic anhydrase and matrix-matalloproteinase inhibitors, respectively (Fig. 1) [8–10]. Additionally, 3-(3,4-dihydroisoquinolin-2(1*H*)-ylsulfonyl)benzoic acid (**6**) was shown to be selective and potent inhibitor of an aldo-keto reductase 1C3 (AKR1C3) [11]. Replacement of the carboxyl group with pyrrolidin-2-one core as compound **7** retained the activity, but with 3-fold less potent than the parent compound **6**. The structure–activity relationship (SAR) results of THIQs **6** and **7** showed that the sulfonamide moiety was critical for AKR1C3 inhibitory activity [12].

AKR1C3, a member of the aldo-keto reductase superfamily of enzymes, plays an important role in stereospecific reduction of carbonyl groups on both steroid and prostaglandin substrates using

* Corresponding author.
E-mail address: ratchanok@swu.ac.th (R. Pingaew).

http://dx.doi.org/10.1016/j.ejmech.2014.05.019
0223-5234/

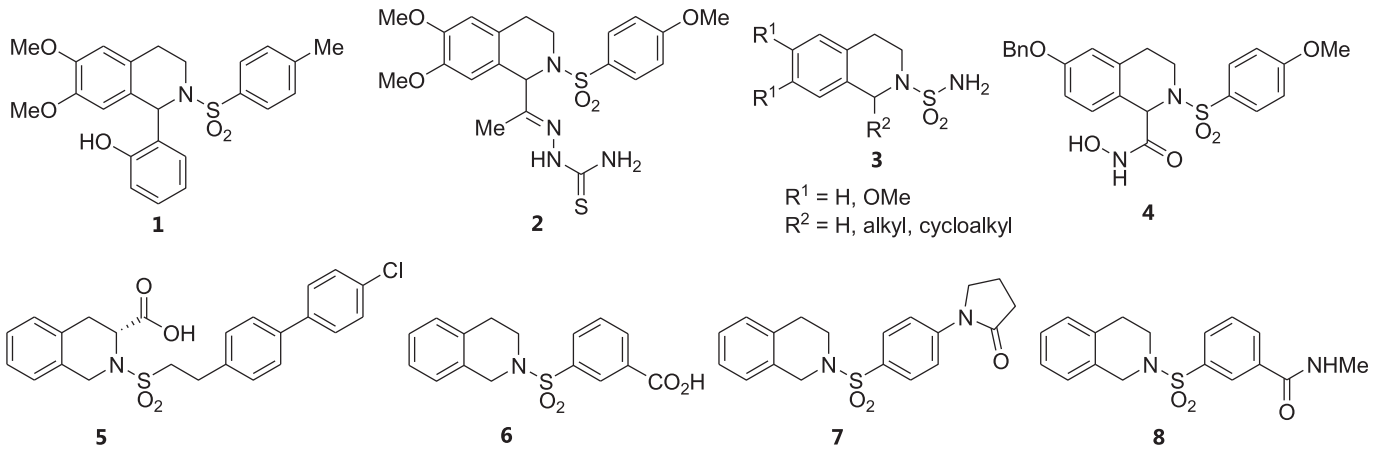

Fig. 1. Representative structures of bioactive *N*-sulfonyl-1,2,3,4-tetrahydroisoquinolines **1**–**8.**

NADPH as a cofactor [13–16]. The reduction products of AKR1C3-promoted reaction such as testosterone, 17β-estradiol, 20α-hydroxy progesterone and $PGF_{2\alpha}$ can stimulate tumor growth, therefore AKR1C3 expression levels are correlated with both hormone-dependent and hormone-independent cancers [15]. AKR1C3 is over-expressed in a number of cancers, particularly, in the prostate and mammary gland where it is responsible for the production of a series of growth-stimulatory steroid hormones. Consequently, inhibition of the catalytic activity renders AKR1C3 as an attractive therapeutic target for treating various types of cancer and for the development of novel anticancer drugs.

Triazole moiety is a common pharmacophore found in a diverse range of biologically active molecules [17,18]. Potential structural features of bioactive triazole include capability of hydrogen bonding, stable to metabolic degradation, high selectivity and less unfavorable reactions. Molecules linking with triazole scaffold are considered to improve their pharmacological activities [19,20]. Importantly, substituted triazole analogs **9**–**12** (Fig. 2) have been used in clinical trials for cancer therapy [17,18]. Recently, our group reported that an open chain analog of *N*-sulfonyl-THIQ bearing triazole, methyl 2-((1-(4-(*N*-phenethylsulfamoyl)phenyl)-1*H*-1,2,3-triazol-4-yl)methoxy)benzoate (**13**), displayed antiproliferative activity against cancer cell lines (e.g., HepG2 and MOLT-3) [20].

The reported bioactive pharmacophores lead to the rational design of new THIQ rigid analogs based on the triazole moiety. As part of our ongoing research, a new series of hybrid molecules containing both THIQ and triazole were designed and synthesized. Thus, target molecules **14**–**33** (Fig. 3) were obtained by the replacement of a phenethylamine moiety of compound **13** with a restricted THIQ ring and by the replacement of a carboxyl group of compound **6** with a triazole ring. A variety of expected novel hybrids were then evaluated for their *in vitro* antiproliferative activity against cancer cell lines and normal cells. Molecular docking of these compounds against AKR1C3 has been carried out.

2. Results and discussion

2.1. Chemistry

Several new *N*-benzenesulfonyl-1,2,3,4-tetrahydroisoquinolines (**14**–**33**) were synthesized using the modified Pictet–Spengler reaction and the Click chemistry approaches as key steps shown in Scheme 1. Initially, treatments of nitrobenzenesulfonamides **34** [7] with paraformaldehyde in refluxing formic acid were smoothly cyclized *via* the modified Pictet–Spengler reaction [6] to furnish 1,2,3,4-tetrahydroisoquinolines **35** [21,22] in good yields. Reduction of the nitro derivatives **35** was performed using stannous chloride in refluxing ethanol to give aminobenzenesulfonamides **36**. Conversion of the amino compounds **36** to the corresponding azidobenzensulfonamides **37** was readily achieved through diazotization

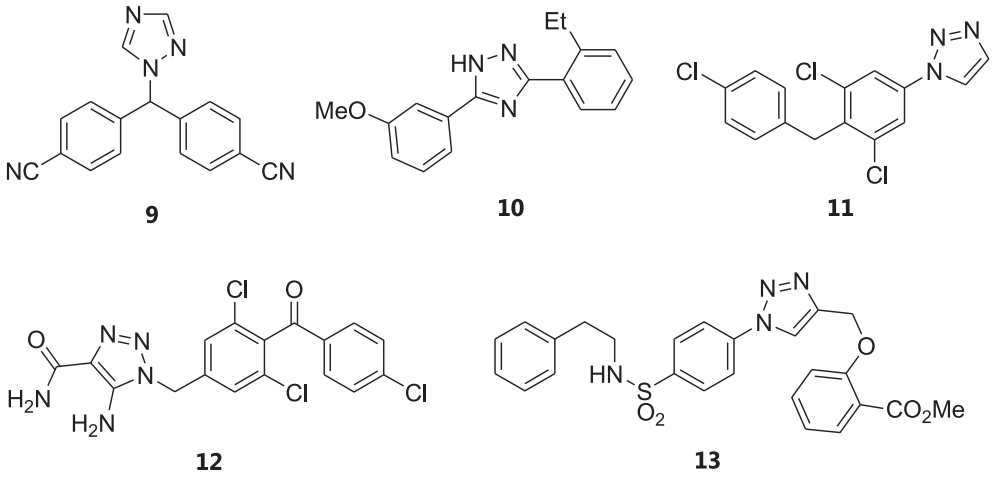

Fig. 2. Representative structures of bioactive triazoles **9**–**13.**

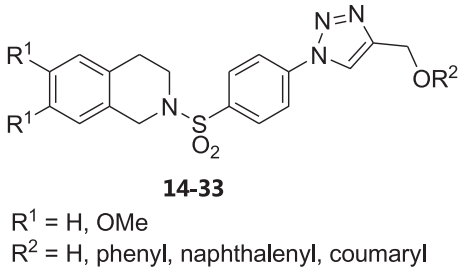

Fig. 3. Synthetic *N*-benzenesulfonyl-1,2,3,4-tetrahydroisoquinoline based triazoles **14**–**33**.

reaction using sodium nitrite in a mixture of glacial acetic acid and concentrated hydrochloric acid in the presence of sodium azide. Finally, cycloaddition reaction (the Click chemistry) of the azides **37** with various alkynes **38** obtaining from alkylation of the appropriate phenol derivatives with propargyl bromide afforded a variety of the desired triazoles **14**–**33** (Scheme 1) in moderate to good yields (45–94%).

Structures of the desired 1,2,3-triazoles **14**–**33** were identified based on their HRMS, IR and NMR spectra. For example, the HRMS-TOF of hydroxymethyltriazole **23** showed its molecular ion $[M+H]^+$ peak at 431.1389 corresponding to the molecular formula of $C_{20}H_{23}N_4O_5S$. The IR spectra of the compound **23** exhibited absorption bands of O–H group at 3280 cm^{-1} and of C=C moiety at 1599 cm^{-1}. The ^1H NMR spectra revealed two triplets at δ 2.78 and 3.33 ppm which were assigned to the methylene protons of C4- and C3-THIQ, respectively. The methylene protons at C1-THIQ ring appeared as a singlet at δ 4.16 ppm whereas two methoxy protons at C6- and C7-positions of the THIQ part appeared as two singlets at δ 3.67 and 3.68 ppm. In addition, the methylene protons of $-CH_2OH$ group were found to be displayed as a doublet at δ 4.62 ppm, and the hydroxyl proton was observed as a triplet at δ 5.41 ppm. Aromatic protons of THIQ ring (H-5 and H-8) displayed as two singlets at δ 6.67 ppm and 6.76 ppm. Two doublets at δ 7.99 and 8.19 ppm with *J* value of 8.8 Hz were attributed to four aromatic protons of benzenesulfonyl moiety at position 2′(6′) and 3′(5′). A singlet of a methine proton of the triazole ring appeared down field chemical shift at δ 8.83 ppm. In the ^{13}C NMR spectra, three methylene carbons (C-1, C-3 and C-4) of THIQ ring were visible at δ 28.0, 44.1 and 47.4 ppm whereas a methylene carbon of $-CH_2OH$ group was observed at δ 55.4 ppm. Two methoxy carbons (at C-6 and C-7) of THIQ ring were noted at 55.9 and 56.0 ppm. Seven quaternary aromatic carbons (ArC) were observed at chemical shift 123.6, 125.2, 136.0, 140.2, 147.8, 148.1 and 150.1 ppm, and seven tertiary aromatic carbons (ArCH) appeared at chemical shift 110.3, 112.3, 120.8 (2ArCH), 121.7 and 129.8 (2ArCH) ppm.

2.2. Biological activity

A series of *N*-benzenesulfonyl-1,2,3,4-tetrahydroisoquinolines (**14**–**33**) (i.e., with or without 6,7-dimethoxy substituents) were preliminarily evaluated *in vitro* as antiproliferative agents against four human cancer cell lines including HuCCA-1 (cholangiocarcinoma), HepG2 (hepatocellular carcinoma), A549 (lung carcinoma) and MOLT-3 (lymphoblastic leukemia) cell lines as summarized in Table 1. These compounds were also tested against the noncancerous (Vero) cell line derived from African green monkey kidney (Table 1). Results showed that substituents (R^1) on the isoquinoline ring and substituents (R^2) on the triazole core play important roles in governing their cytotoxicities. SAR studies of the tested compounds are discussed hereafter.

It was observed that in a series of 1,2,3,4-tetrahydroisoquinoline (**14**–**22**) without 6,7-dimethoxy substituents (R^1 = H), the triazole (**14**) bearing hydroxymethyl substituent (R^2 = H) showed selective inhibition against HuCCA-1 cells. The cytotoxic activity of compound **14** in HuCCA-1 cells was lost when the H atom (R^2) of the OH group was replaced with a phenyl group as seen for compound **15**. On the other hand, the cytotoxic activity of compound **15** showed

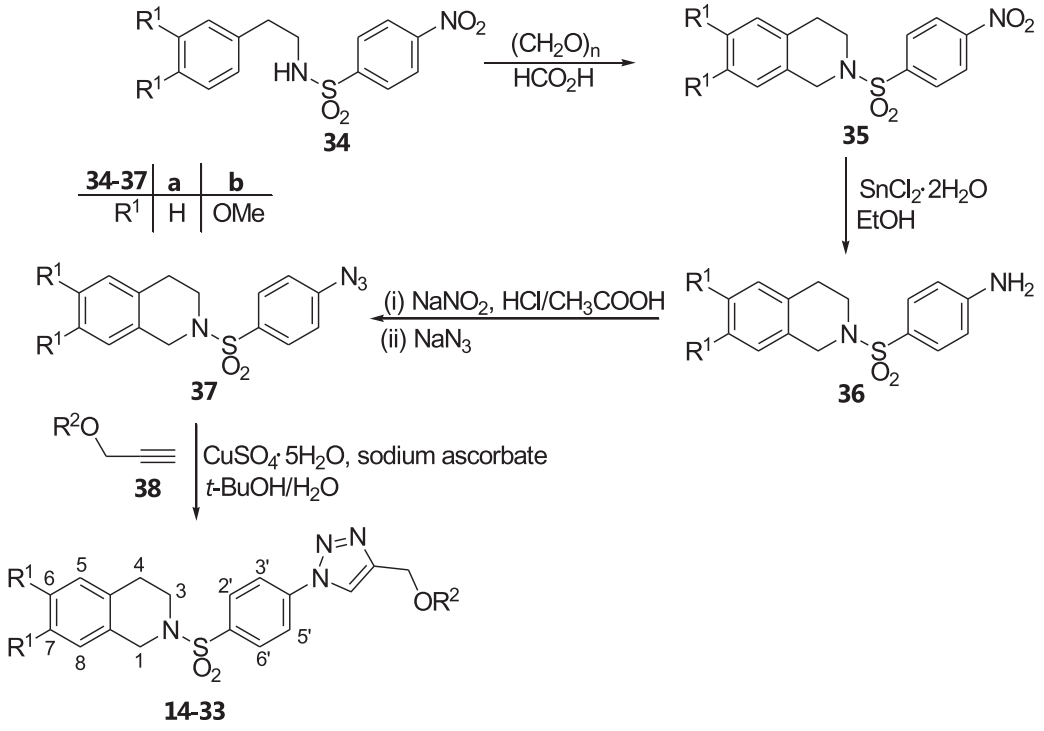

Scheme 1. Synthesis of *N*-benzenesulfonyl-1,2,3,4-tetrahydroisoquinoline based triazoles **14**–**33** through the Pictet–Spengler reaction and the Click reaction.

Table 1
Cytotoxic activity (IC_{50}, μM) of compounds (**14**–**33**) against four cancer cell lines and Vero cell line.

Compound	R^1	R^2	Cancer cell lines[a]				Vero cell line
			HuCCA-1	HepG2	A549	MOLT-3	
14	H	H	51.35 ± 5.66	Non-cytotoxic	Non-cytotoxic	Non-cytotoxic	Non-cytotoxic
15	H		Non-cytotoxic	6.50 ± 0.14	Non-cytotoxic	Non-cytotoxic	Non-cytotoxic
16	H	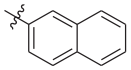	Non-cytotoxic	60.48 ± 14.14	Non-cytotoxic	Non-cytotoxic	Non-cytotoxic
17	H	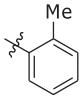	Non-cytotoxic	Non-cytotoxic	66.30 ± 0.70	Non-cytotoxic	Non-cytotoxic
18	H	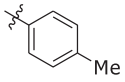	Non-cytotoxic	Non-cytotoxic	Non-cytotoxic	Non-cytotoxic	Non-cytotoxic
19	H	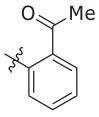	30.16 ± 4.07	19.12 ± 3.06	14.90 ± 1.02	21.86 ± 3.67	Non-cytotoxic
20	H	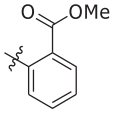	0.63 ± 0.04	12.36 ± 1.97	0.57 ± 0.02	18.63 ± 1.62	4.98
21	H	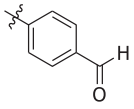	Non-cytotoxic	5.27 ± 0.71	59.07 ± 11.31	Non-cytotoxic	Non-cytotoxic
22	H	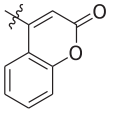	24.80 ± 2.19	Non-cytotoxic	25.29 ± 10.78	80.78 ± 10.23	28.58
23	OMe	H	72.0 ± 10.54	31.79 ± 2.89	41.04 ± 9.40	Non-cytotoxic	Non-cytotoxic
24	OMe		Non-cytotoxic	2.57 ± 0.99	Non-cytotoxic	Non-cytotoxic	Non-cytotoxic
25	OMe	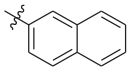	Non-cytotoxic	1.26 ± 0.42	Non-cytotoxic	36.35 ± 1.36	Non-cytotoxic
26	OMe	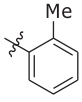	39.71 ± 1.48	1.48 ± 0.61	27.21 ± 1.77	Non-cytotoxic	Non-cytotoxic
27	OMe	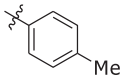	Non-cytotoxic	0.56 ± 0.01	Non-cytotoxic	Non-cytotoxic	Non-cytotoxic
28	OMe	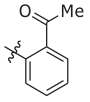	Non-cytotoxic	Non-cytotoxic	Non-cytotoxic	Non-cytotoxic	37.23
29	OMe	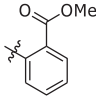	4.79 ± 0.28	3.37 ± 0.96	8.43 ± 2.79	11.74 ± 4.97	2.82
30	OMe	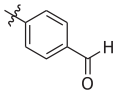	31.09 ± 8.91	12.49 ± 2.47	31.84 ± 8.13	34.12 ± 0.97	Non-cytotoxic

(*continued on next page*)

Table 1 (*continued*)

Compound	R^1	R^2	Cancer cell lines[a]				Vero cell line
			HuCCA-1	HepG2	A549	MOLT-3	
31	OMe	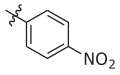	Non-cytotoxic	Non-cytotoxic	Non-cytotoxic	Non-cytotoxic	Non-cytotoxic
32	OMe	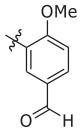	76.15 ± 1.77	41.36 ± 2.89	31.91 ± 9.76	5.82 ± 0.85	Non-cytotoxic
33	OMe	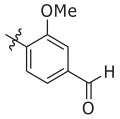	39.98 ± 4.03	Non-cytotoxic	Non-cytotoxic	5.50 ± 0.61	Non-cytotoxic
Etoposide[b]			ND	30.16 ± 0.50	ND	0.051 ± 0.002	ND
Doxorubicin[b]			0.83 ± 0.07	0.79 ± 0.08	0.44 ± 0.01	ND	ND
Ellipticine[b]			ND	ND	ND	ND	1.94

Non-cytotoxic = IC_{50} > 50 μg/mL.
Vero cell line = African green monkey kidney cell line.
ND not determined.
[a] Cancer cell lines comprise the following: HuCCA-1 human cholangiocarcinoma cell line, HepG2 human hepatocellular carcinoma cell line, A549 human lung carcinoma cell line, MOLT-3 human lymphoblastic leukemia cell line.
[b] Etoposide, doxorubicin and ellipticine were used as reference drugs.

remarkably enhanced effect (IC_{50} = 6.50 μM) in HepG2 cells. Replacement of the phenyl ring (R^2) with the naphthalenyl ring as observed in compound **16** afforded a decrease in the cytotoxic potency against HepG2. *o*-Tolyloxymethyl analog (**17**) was shown to be a selective cytotoxic compound against A549 cells. However, isomeric effect of tolyl group on the cytotoxic activity was seen in triazole **18** bearing *p*-tolyl group (R^2) in which its activity was totally lost. Significantly, phenyl groups (R^2) possessing *ortho*-substituents on the phenyl ring such as COMe (**19**) and CO_2Me (**20**) displayed cytotoxic activities toward all tested cancer cell lines in which methylbenzoate (**20**) was shown to be the most potent compound having comparable IC_{50} value (0.57 μM) with that of the control drug, doxorubicin (IC_{50} = 0.44 μM), in A549 cells. It was also found that the ester analog **20** was the most active compound (IC_{50} = 0.63 μM) against HuCCA-1 cells and exerted higher activity than that of the doxorubicin. Enhancement in anticancer activity of the phenoxytriazole compound **15** ($R^2 = C_6H_5$) against HepG2 and A549 cells was observed when a formyl group was introduced at the *para* position of the phenyl moiety as noted for compound **21**. Apparently, the phenoxy compound (**15**) and its derivatives bearing ketone (**19**), ester (**20**) and aldehyde (**21**) groups displayed high cytotoxic activity against HepG2 cells as compared to the reference drug, etoposide. When the phenyl group of compound **15** was replaced with a coumaryl ring as found in compound **22**, the enhanced cytotoxic potency was observed against HuCCA-1, A549 and MOLT-3 cell lines whereas the activity was lost in HepG2 cells.

In a 6,7-dimethoxy-1,2,3,4-tetrahydroisoquinoline series (**23**–**33**, R^1 = OMe), the hydroxymethyltriazole (**23**) (R^2 = H) was shown to be active against HuCCA-1, HepG2 and A549 cell lines. Such cytotoxic activity in HuCCA-1 and A549 cells of compound **23** was lost when the H atom was replaced with a phenyl group as seen for compound **24**. Cytotoxic activity against HepG2 cells was distinctively enhanced when the H atom of **23** was substituted with phenyl (**24**), naphthalenyl (**25**) and tolyl (**26**, **27**) groups. Significant results showed that *p*-tolyloxy compound (**27**) displayed selective inhibition and exerted the highest cytotoxic activity against HepG2 cells with IC_{50} of 0.56 μM (i.e., 53.9-fold and 1.4-fold stronger activity than etoposide and doxorubicin, respectively). Obviously, it was found that triazoles bearing the phenoxymethyl (**24**) moiety and phenoxymethyl (**26**, **27**, **29**, **30**) with substituents (CH_3, CO_2Me, CHO) on the phenyl ring as well as naphthalenoxymethyl (**25**) exhibited superior inhibitory potency toward HepG2 cells than that of the etoposide. The order of decreasing cytotoxic potency of these cytotoxic triazoles was shown by the following trend: **27** > **25** > **26** > **29** > **30**. Inhibition effect in HepG2 cells of *p*-tolyloxymethyltriazole (**27**) was found to decrease when methyl group on the phenyl ring was replaced with polar substituents (i.e., COMe, CO_2Me, CHO and NO_2). At this point, it was suggested that lipophilic groups, thus seems to be important sites responsible for strong cytotoxic activity as observed in HepG2 cells. Phenoxymethyl compounds constituting methyl ester (**29**) and formyl (**30**) groups on the phenyl ring were found to be active towards all of the tested cancer cell lines whereas compounds with acetylphenyl (**28**) and nitrophenyl (**31**) moieties displayed no cytotoxic activity toward all of the tested cells. Furthermore, additional introduction of methoxyl to the phenyl moiety containing *m*- and *p*-formyl groups as indicated by compounds **32** and **33** led to enhanced cytotoxic activity against MOLT-3 cell line.

Interestingly, most triazole compounds were shown to be non-cytotoxic toward normal cells except for triazole derivatives having methyl esters (**20**, **29**), coumaryl (**22**) and acetyl (**28**) substituents.

SAR analysis revealed that substituents (R^1 and R^2) on the target triazoles play a crucial role in governing their anticancer activity. The strongest activities against HuCCA-1 and A549 cells were noted for compounds bearing polar substituents (R^2) such as triazole ester **20** (R^1 = H, $R^2 = C_6H_4$–CO_2Me-*o*). Promisingly, compounds having high lipophilic substituents (R^1 and R^2), particularly *p*-tolyl triazole **27** (R^1 = OMe, $R^2 = C_6H_4$–Me-*p*) provided the most potent anticancer activity against HepG2 cells without affecting the normal cell line. It was conceivable that such difference in potency and selectivity of compounds in exerting anticancer activity was dependent upon the functionality of their R^1 and R^2 substituents. The strongest activity (HuCCA-1 and A549 cells) may require the compound (**20**) to have polar (CO) electrophilic center for

interacting with cellular nucleophiles. For higher potency in HepG2 cells, higher hydrophobic effect such as those afforded by the tolyl group (**27**) may be involved in binding with the hydrophobic area of the target site.

2.3. Molecular docking

A search for the putative target of 1,2,3,4-tetrahydroisoquinoline-triazoles investigated herein was carried out using the promising triazole analogs **20** and **27** as the query molecules in PubChem. It was revealed that 4-phenylpyrrolidine-2-one analog of 1,2,3,4-tetrahydroisoquinoline (**7**) provided nanomolar potency against AKR1C3 with IC_{50} values of 42 and 52 nM as elucidated by two separate bioactivity experiments [11,12]. Molecular docking was performed as to evaluate the binding modalities of the 1,2,3,4-tetrahydroisoquinoline-triazoles against AKR1C3. The results suggested that all 1,2,3,4-tetrahydroisoquinoline-triazole analogs (**14**–**33**) could snugly occupy the active site of AKR1C3 (Fig. 4) with binding energies in the range of −9.5 to −14.5 kcal/mol (Table 2). It was observed that many of the 1,2,3,4-tetrahydroisoquinoline-triazole analogs afforded binding energy lower than the co-complexed ligand found in the crystal structure, 3-(3,4-dihydroisoquinolin-2(1*H*)-ylsulfonyl)-*N*-methylbenzamide **8**, which provided binding energy of −11.0 kcal/mol indicating possibly higher potency for AKR1C3 inhibition.

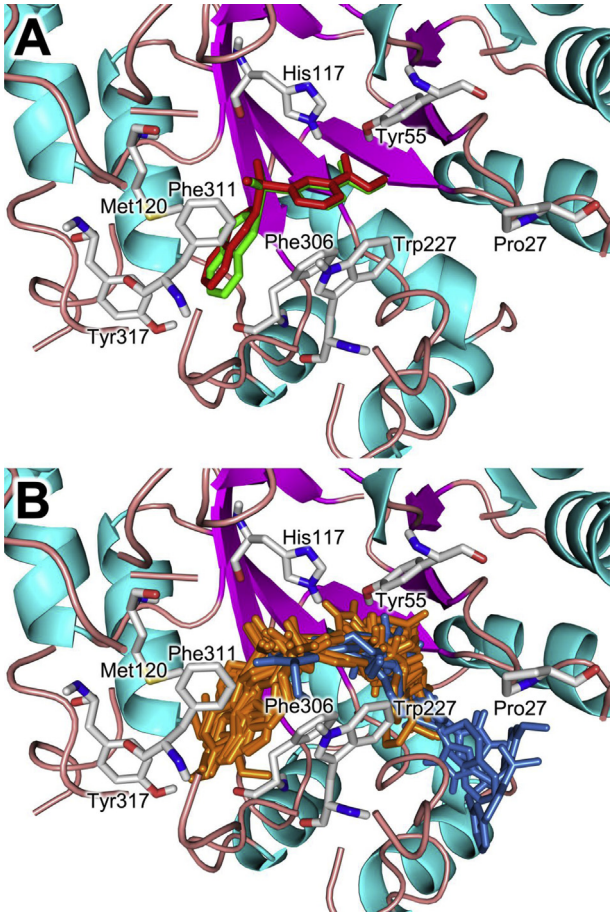

Fig. 4. Molecular docking of tetrahydroisoquinoline-triazole derivatives to AKR1C3. Re-docking of the co-crystallized ligand 3-(3,4-dihydroisoquinolin-2(1*H*)-ylsulfonyl)-*N*-methylbenzamide **8** yielded RMSD of 0.692 Å (A). Poses of docked tetrahydroisoquinoline-triazole derivatives are shown inside the binding cavity (B).

Table 2
Binding energy of 1,2,3,4-tetrahydroisoquinoline-triazole derivatives (**14**–**33**).

Compound	Binding energy (Kcal/mol)	Compound	Binding energy (kcal/mol)
14	−11.1	**24**	−10.1
15	−12.8	**25**	−12.7
16	−14.5	**26**	−11.7
17	−13.2	**27**	−11.5
18	−10.8	**28**	−10.0
19	−13.2	**29**	−11.2
20	−13.1	**30**	−11.3
21	−12.9	**31**	−11.7
22	−14.5	**32**	−11.5
23	−9.5	**33**	−11.1
8[a]	−11.0		

[a] 3-(3,4-Dihydroisoquinolin-2(1*H*)-ylsulfonyl)-*N*-methylbenzamide (**8**) is the co-crystallized ligand found in the crystal structure of AKR1C3.

Molecular modeling analysis of the crystal structure revealed that the co-complexed inhibitor **8**, binds the active site of AKR1C3 *via* hydrogen bonding of amide oxygen to Tyr55 and His117 while the phenyl group engages in hydrophobic interaction with Leu54 and forms π-π stacking with Trp227. The 1,2,3,4-tetrahydroisoquinoline moiety of **8** occupies the hydrophobic pocket inside the active site bounded by Met120, Phe306, Phe311 and Tyr317 residues (Fig. 5A). The triazole **20** could plausibly bind the active site of AKR1C3 with a similar modality as deduced from its docked conformer, particularly the 1,2,3,4-tetrahydroisoquinoline moiety of compound **20** sits inside the hydrophobic pocket formed by Met120, Phe311 and Phe306 residues whereas the phenyl ring (next to the sulfonyl group) is located in a pocket defined by Phe306 and Tyr216 residues. It was observed that the methoxy group of ester (R^2) at the other end of the compound is responsible for hydrogen bond formation with Tyr55. Moreover, compound **20** was found to also engage in hydrogen bonding with Gln222 (using phenoxy O-atom), π-stacking with Tyr24 (using the triazole ring) and hydrophobic interaction with Leu268 and Lys270 (using phenyl ring of R^2 substituent) as shown in Fig. 5B. Interestingly, compound **27**, which exerts specific activity towards the HepG2 cell line, was shown to interact with AKR1C3 through a different mechanism (Fig. 5C). Particularly, the methoxy substituent at the R^1 position sterically hinders the 1,2,3,4-tetrahydroisoquinoline moiety in occupying the hydrophobic pocket as defined by Met120, Phe306 and Phe311. However, the *p*-tolyl substituent at the R^2 position counters the previously mentioned moiety by allowing the ligand to occupy the aforementioned pocket. This instance enabled the triazole ring and the adjacent phenyl ring of sulfonamide **27** to form π-π stacking with Phe306 and Tyr216. Such interaction was strengthen by a hydrogen bonding network formed between the sulfonyl oxygen and Tyr55 as well as the between the oxygen atom of two methoxy substituents at R^1 positions to Lys270 and Ser221.

Taken together, the docking results support the viewpoint that AKR1C3 is a plausible target of 1,2,3,4-tetrahydroisoquinoline-triazoles for which it was shown to interact strongly. It is notable that substituents (R^1 and R^2) on the triazoles (**14**–**33**) are crucial for binding the active site of AKR1C3. Most THIQs without 6,7-dimethoxy substituents (R^1 = H) had lower binding energy than the corresponding compounds with 6,7-dimethoxy substituents (R^1 = OMe). However, the lowest binding energy (−14.5 kcal/mol) was observed for compounds having more bulky planar lipophilic groups (R^2) such as those found in naphthalenyl (**16**) and coumaryl (**22**). Such results could be reasonably explained that the chemical properties of R^1 and R^2 governed the compounds in interacting or fitting inside the hydrophobic pocket areas of AKR1C3.

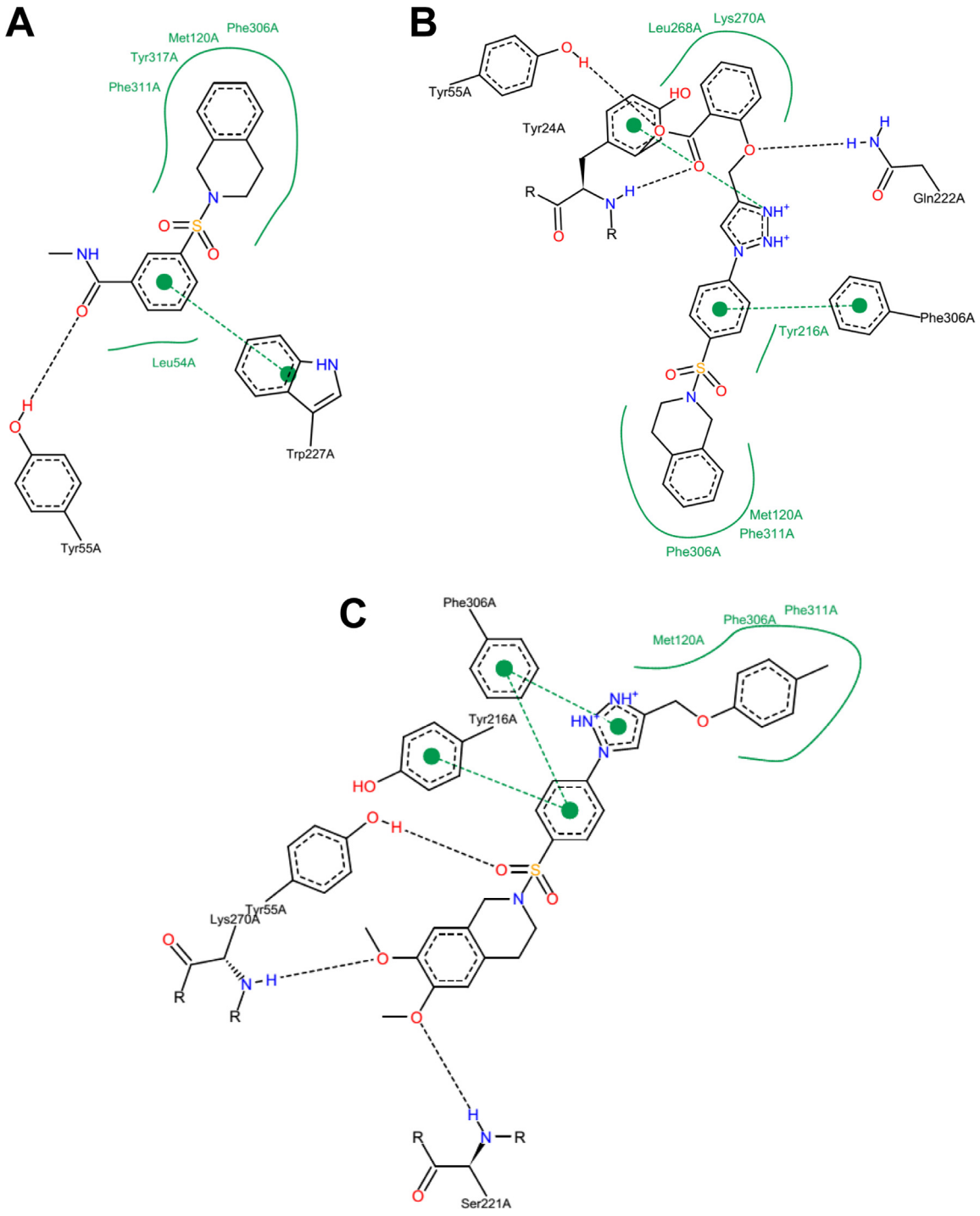

Fig. 5. 2D ligand–protein interaction schemes of the co-crystallized ligand 3-(3,4-dihydroisoquinolin-2(1*H*)-ylsulfonyl)-*N*-methylbenzamide **8** (A), the docked pose of compound **20** (B) and the docked pose of compound **27** (C).

3. Conclusions

A novel series of tetrahydroisoquinoline-triazole hybrids (**14**–**33**) have been synthesized *via* two key steps using the modified Pictet–Spengler reaction and the click reaction. Their anti-proliferative activity against four cancer (HuCCA-1, HepG2, A549 and MOLT-3) cell lines and molecular docking with AKR1C3 were studied. It was observed that triazole esters (**20** and **29**) with R^2 = methylbenzoate were active toward all of the tested cell lines in which the ester analog **20** was shown to be the most potent compound against HuCCA-1 (IC_{50} = 0.63 μM) and A549 (IC_{50} = 0.57 μM) cell lines. The triazole **27** containing 6,7-dimethoxy substituent (R^1) on the isoquinoline core and *p*-tolyl group (R^2) on the triazole part was a promising compound showing the strongest and selective cytotoxicity in HepG2 cells (IC_{50} 0.56 μM) without affecting the normal cell line. The potent and selective action of compounds may be a direct function of their substituents at R^1 and R^2 positions. Activities against HuCCA-1 and A549 cells may require the compound (**20**) to have polar electrophilic center in interacting with cellular nucleophiles. The potent

activity against HepG2 cells may be rationalized to be due to the hydrophobic group (**27**) in which it binds the hydrophobic region of the target site of action. Furthermore, molecular docking study indicated that all of the investigated triazoles could snugly occupy the active site of AKR1C3, which had been identified to be a plausible target site of such compounds.

4. Experimental section

4.1. Chemistry

Column chromatography was carried out using silica gel 60 (70–230 mesh ASTM). Analytical thin-layer chromatography (TLC) was performed with silica gel 60 F254 aluminum sheets. ^{1}H- and ^{13}C-NMR spectra were recorded on a Bruker AVANCE 300 NMR spectrometer (operating at 300 MHz for 1H and 75 MHz for ^{13}C). The following standard abbreviations were used for signal multiplicities: singlet (s), doublet (d), triplet (t), quartet (q), multiplet (m), and broad (br). FTIR spectra were obtained using a universal attenuated total reflectance attached on a Perkin–Elmer Spectrum One spectrometer. Mass spectra were recorded on a Bruker Daltonics (microTOF). Melting points were determined using a Griffin melting point apparatus and were uncorrected.

4.2. General procedure for the synthesis of 1,2,3,4-tetrahydroisoquinolines (**35**)

A mixture of sulfonamide **34** (0.67 mmol) and paraformaldehyde (0.72 mmol) in formic acid (15 mL) was refluxed for 2 h, and then allowed to cool to room temperature. The reaction mixture was added to 30 mL of water, and the product was extracted with CH_2Cl_2 (2 × 30 mL). Combined extracts were washed with saturated aqueous $NaHCO_3$, dried (anh. Na_2SO_4) and evaporated to dryness under reduced pressure. The crude product was recrystallized from methanol.

^{1}H NMR of 2-((4-nitrophenyl)sulfonyl)-1,2,3,4-tetrahydroisoquinoline (**35a**) and 6,7-dimethoxy-2-((4-nitrophenyl)sulfonyl)-1,2,3,4-tetrahydroisoquinoline (**35b**) were consistent with those reported in the literatures [21,22].

4.3. General procedure for the synthesis of 1,2,3,4-tetrahydroisoquinolines (**36**)

A mixture of nitroisoquinoline **35** (4 mmol) and $SnCl_2 \cdot 2H_2O$ (20 mmol) in absolute ethanol (20 mL) was stirred under reflux for 4 h then concentrated under reduced pressure. Water (20 mL) was added and extracted with EtOAc (3 × 20 mL). The organic extracts were combined and washed with water (20 mL) and brine (20 mL). The organic layer was dried over anhydrous sodium sulfate, filtered and concentrated. The crude product was purified using silica gel column chromatography and eluted with acetone:hexane (3:7).

4.3.1. 2-((4-Aminophenyl)sulfonyl)-1,2,3,4-tetrahydroisoquinoline (**36a**)

Pale yellow solid. 82%. mp 175–176 °C (175.0–175.5 °C [23]). IR (UATR) cm^{-1}: 3454, 3362, 1591, 1503, 1324, 1155. ^{1}H NMR (300 MHz, DMSO-d_6) δ 2.84 (t, J = 5.8 Hz, 2H, C4–*H*), 3.16 (t, J = 5.8 Hz, 2H, C3–*H*), 4.06 (s, 2H, C1–*H*), 6.08 (s, 2H, N*H*$_2$), 6.64 (d, J = 8.7 Hz, 2H, Ar*H*), 7.05–7.18 (m, 4H, Ar*H*), 7.44 (d, J = 8.7 Hz, 2H, Ar*H*). ^{13}C NMR (75 MHz, DMSO-d_6) δ 28.1, 43.6, 47.4, 112.7, 120.0, 126.0, 126.4, 126.5, 128.6, 129.5, 131.9, 133.1, 153.2. HRMS-TOF: m/z [M+Na]$^+$ 311.0829 (Calcd for $C_{15}H_{16}N_2NaO_2S$: 311.0825).

4.3.2. 2-((4-Aminophenyl)sulfonyl)-6,7-dimethoxy-1,2,3,4-tetrahydroisoquinoline (**36b**)

Pale yellow solid. 80%. mp 185–186 °C. IR (UATR) cm^{-1}: 3468, 3372, 1596, 1518, 1316, 1153. ^{1}H NMR (300 MHz, DMSO-d_6) δ 2.75 (t, J = 5.9 Hz, 2H, C4–*H*), 3.12 (t, J = 5.9 Hz, 2H, C3–*H*), 3.68 (s, 6H, 2 × OC*H*$_3$), 3.92 (s, 2H, C1–*H*), 6.65 (d, J = 8.4 Hz, 2H, Ar*H*), 6.66 (s, 1H, Ar*H*), 6.73 (s, 1H, Ar*H*), 7.42 (d, J = 8.4 Hz, 2H, Ar*H*). ^{13}C NMR (75 MHz, DMSO-d_6) δ 28.2, 44.2, 47.6, 55.9, 110.3, 112.1, 113.2, 120.4, 123.9, 125.2, 130.0, 147.7, 147.9, 153.6. HRMS-TOF: m/z [M+Na]$^+$ 371.1035 (Calcd for $C_{17}H_{20}N_2NaO_4S$: 371.1036).

4.4. General procedure for the synthesis of 2-((4-azidophenyl)sulfonyl)-1,2,3,4-tetrahydroisoquinolines (**37**)

To a cold solution of amine **36** (3 mmol) in HCl:CH_3COOH (3:3 mL) at 0 °C, a solution of sodium nitrite (9 mmol) in water (5 mL) was added. The stirred reaction mixture was maintained for 15 min and then added dropwise a solution of sodium azide (9 mmol) in water (5 mL). The reaction mixture was allowed to stir at room temperature for 0.5 h, then the precipitate was filtered and washed with cold water. The crude product was purified using silica gel column chromatography and eluted with acetone:hexane (2:8).

4.4.1. 2-((4-Azidophenyl)sulfonyl)-1,2,3,4-tetrahydroisoquinoline (**37a**)

Pale yellow solid. 94%. mp 126–127 °C. IR (UATR) cm^{-1}: 2129, 2099, 1589, 1489, 1337, 1287, 1163. ^{1}H NMR (300 MHz, $CDCl_3$) δ 2.90 (t, J = 6.0 Hz, 2H, C4–*H*), 3.36 (t, J = 6.0 Hz, 2H, C3–*H*), 4.25 (s, 2H, C1–*H*), 6.96–7.18 (m, 6H, Ar*H*), 7.80 (d, J = 8.7 Hz, 2H, Ar*H*). ^{13}C NMR (75 MHz, $CDCl_3$) δ 28.8, 43.7, 47.5, 119.4, 126.3, 126.4, 126.9, 128.8, 129.6, 131.4, 132.9, 133.0, 144.9. HRMS-TOF: m/z [M+Na]$^+$ 337.0726 (Calcd for $C_{15}H_{14}N_4NaO_2S$: 337.0730).

4.4.2. 2-((4-Azidophenyl)sulfonyl)-6,7-dimethoxy-1,2,3,4-tetrahydroisoquinoline (**37b**)

Pale yellow solid. 85%. mp 145–146 °C. IR (UATR) cm^{-1}: 2126, 2100, 1588, 1519, 1345, 1284, 1163. ^{1}H NMR (300 MHz, $CDCl_3$) δ 2.81 (t, J = 5.9 Hz, 2H, C4–*H*), 3.33 (t, J = 5.9 Hz, 2H, C3–*H*), 3.80 (s, 6H, 2 × OC*H*$_3$), 4.17 (s, 2H, C1–*H*), 6.48 (s, 1H, Ar*H*), 6.53 (s, 1H, Ar*H*), 7.12 (d, J = 8.7 Hz, 2H, Ar*H*), 7.79 (d, J = 8.7 Hz, 2H, Ar*H*). ^{13}C NMR (75 MHz, $CDCl_3$) δ 28.3, 43.7, 47.2, 55.9, 56.0, 108.9, 111.4, 119.4, 123.2, 124.9, 129.5, 132.8, 144.9, 147.8, 148.0. HRMS-TOF: m/z [M+Na]$^+$ 397.0946 (Calcd for $C_{17}H_{18}N_4NaO_4S$: 397.0941).

4.5. General procedure for the synthesis of propynyloxy derivatives (**38**)

A propargyl bromide (2.4 mmol) was added to a suspension of an appropriate phenol (2 mmol) and potassium carbonate (4 mmol) in acetone (15 mL). The suspension was heated to reflux for 2–6 h (monitored by TLC). The reaction was allowed to cool and then concentrated under reduced pressure. Water (30 mL) was added and extracted with CH_2Cl_2 (3 × 30 mL). The organic extracts were combined and washed with water (20 mL) and brine (20 mL). The organic layer was dried over anhydrous sodium sulfate, filtered and concentrated. The crude product was purified by column chromatography.

^{1}H NMR spectra of propynyloxy derivatives (**38**) including (2-propynyloxy)benzene [24], 2-(2-propynyloxy)naphthalene [25], 1-methyl-2-(2-propynyloxy)benzene [26], 1-methyl-4-(2-propynyloxy)benzene [27], 1-(2-(prop-2-ynyloxy)phenyl)ethanone [28], methyl 2-(2-propynyloxy)benzoate [29], 4-(2-propynyloxy) benzaldehyde [28], 4-(propynyloxy)-2*H*-chromen-2-one [30], 1-nitro-4-(2-propynyloxy)benzene [25], 4-methoxy-3-(2-

propynyloxy)benzaldehyde [31] and 3-methoxy-4-(2-propynyloxy) [31] were consistent with those reported in the literatures.

4.6. General procedure for the synthesis of 4-(4-(substituted)-1H-1,2,3-triazol-1-yl)-N-phenethylbenzenesulfonamides (**14**–**33**)

To a stirred solution of azido **37** (0.2 mmol) and alkyne **38** (0.2 mmol) in *t*-BuOH:H_2O (3:3 mL), $CuSO_4 \cdot 5H_2O$ (0.2 mmol) and ascorbic acid (0.5 mmol) were added. The reaction mixture was stirred at room temperature for 2–12 h (monitored by TLC), then concentrated under reduced pressure. The residue was added water (10 mL) and extracted with dichloromethane (3 × 20 mL). The combined organic phases were washed with water (20 mL), dried over anhydrous sodium sulfate and evaporated to dryness. The crude product was purified using silica gel column chromatography and eluted with methanol:dichloromethane (1:50).

4.6.1. (1-(4-((3,4-Dihydroisoquinolin-2(1H)-yl)sulfonyl)phenyl)-1H-1,2,3-triazol-4-yl)methanol (**14**)

White solid. 45%. mp 111–112 °C. IR (UATR) cm^{-1}: 3280, 1597, 1503, 1336, 1243, 1161. ^1H NMR (300 MHz, DMSO-d_6) δ 2.87 (br t, 2H, C4–*H*), 3.35 (br t, 2H, C3–*H*), 4.27 (s, 2H, C1–*H*), 4.62 (d, J = 5.4 Hz, 2H, CH_2OH), 5.41 (t, J = 5.4 Hz, 1H, CH_2O*H*), 7.05–7.20 (m, 4H, Ar*H*), 8.03 (d, J = 8.7 Hz, 2H, Ar*H*), 7.97 (d, J = 8.6 Hz, 2H, Ar*H*), 8.85 (s, 1H, C*H*N). ^{13}C NMR (75 MHz, DMSO-d_6) δ 28.4, 44.0, 47.7, 55.4, 120.8, 121.7, 126.6, 126.9, 127.2, 129.1, 129.8, 132.0, 133.4, 136.0, 140.2, 150.1. HRMS-TOF: m/z $[M+Na]^+$ 393.0988 (Calcd for $C_{18}H_{18}N_4NaO_3S$: 393.0992).

4.6.2. 2-((4-(4-(Phenoxymethyl)-1H-1,2,3-triazol-1-yl)phenyl)sulfonyl)-1,2,3,4-tetrahydroisoquinoline (**15**)

White solid. 84%. mp 186–187 °C. IR (UATR) cm^{-1}: 1598, 1497, 1337, 1243, 1162. ^1H NMR (300 MHz, $CDCl_3$) δ 2.92 (t, J = 6.0 Hz, 2H, C4–*H*), 3.43 (t, J = 6.0 Hz, 2H, C3–*H*), 4.32 (s, 2H, C1–*H*), 5.29 (s, 2H, CH_2O), 6.94–7.33 (m, 9H, Ar*H*), 7.91 (d, J = 8.8 Hz, 2H, Ar*H*), 7.98 (d, J = 8.8 Hz, 2H, Ar*H*), 8.10 (s, 1H, C*H*N). ^{13}C NMR (75 MHz, $CDCl_3$) δ 28.7, 43.7, 47.5, 61.9, 114.7, 120.6, 121.5, 126.3, 126.5, 127.0, 128.9, 129.4, 129.7, 131.2, 132.9, 137.1, 139.9, 145.9, 158.0. HRMS-TOF: m/z $[M+Na]^+$ 469.1292 (Calcd for $C_{24}H_{22}N_4NaO_3S$: 469.1305).

4.6.3. 2-((4-(4-((Naphthalen-2-yloxy)methyl)-1H-1,2,3-triazol-1-yl)phenyl)sulfonyl)-1,2,3,4-tetrahydroisoquinoline (**16**)

White solid. 52%. mp 241–242 °C. IR (UATR) cm^{-1}: 1597, 1508, 1337, 1243, 1161. ^1H NMR (300 MHz, $CDCl_3$) δ 2.91 (t, J = 5.6 Hz, 2H, C4–*H*), 3.43 (t, J = 5.8 Hz, 2H, C3–*H*), 4.32 (s, 2H, C1–*H*), 5.26 (s, 2H, CH_2O), 6.85–7.18 (m, 11H, Ar*H*), 7.91 (d, J = 8.6 Hz, 2H, Ar*H*), 7.98 (d, J = 8.6 Hz, 2H, Ar*H*), 8.09 (s, 1H, C*H*N). ^{13}C NMR (75 MHz, $CDCl_3$) δ 28.7, 43.7, 47.5, 62.1, 114.6, 120.6, 126.3, 126.5, 127.0, 128.9, 129.4, 130.1, 130.9, 131.2, 132.9, 137.2, 139.9, 146.1, 156.0. HRMS-TOF: m/z $[M+H]^+$ 497.1647 (Calcd for $C_{28}H_{25}N_4O_3S$: 497.1653).

4.6.4. 2-((4-(4-((o-Tolyloxy)methyl)-1H-1,2,3-triazol-1-yl)phenyl)sulfonyl)-1,2,3,4-tetrahydroisoquinoline (**17**)

White solid. 77%. mp 168–169 °C. IR (UATR) cm^{-1}: 1596, 1495, 1339, 1240, 1164. ^1H NMR (300 MHz, $CDCl_3$) δ 2.28 (s, 3H, CH_3), 2.96 (t, J = 5.9 Hz, 2H, C4–*H*), 3.47 (t, J = 5.9 Hz, 2H, C3–*H*), 4.36 (s, 2H, C1–*H*), 5.34 (s, 2H, CH_2O), 6.90–7.24 (m, 8H, Ar*H*), 7.95 (d, J = 8.9 Hz, 2H, Ar*H*), 8.03 (d, J = 8.8 Hz, 2H, Ar*H*), 8.11 (s, 1H, C*H*N). ^{13}C NMR (75 MHz, $CDCl_3$) δ 16.3, 28.7, 43.7, 47.5, 62.2, 111.5, 120.4, 120.6, 121.3, 126.3, 126.5, 127.0, 128.9, 129.4, 131.0, 131.2, 132.9, 139.9, 146.3, 156.2. HRMS-TOF: m/z $[M+H]^+$ 461.1637 (Calcd for $C_{25}H_{25}N_4O_3S$: 461.1653).

4.6.5. 2-((4-(4-((p-Tolyloxy)methyl)-1H-1,2,3-triazol-1-yl)phenyl)sulfonyl)-1,2,3,4-tetrahydroisoquinoline (**18**)

White solid. 88%. mp 196–197 °C. IR (UATR) cm^{-1}: 1598, 1512, 1338, 1244, 1162. ^1H NMR (300 MHz, $CDCl_3$) δ 2.27 (s, 3H, CH_3), 2.92 (t, J = 6.0 Hz, 2H, C4–*H*), 3.43 (t, J = 6.0 Hz, 2H, C3–*H*), 4.32 (s, 2H, C1–*H*), 5.26 (s, 2H, CH_2O), 6.89 (d, J = 8.5 Hz, 2H, Ar*H*), 7.00–7.16 (m, 6H, Ar*H*), 7.90 (d, J = 8.8 Hz, 2H, Ar*H*), 7.98 (d, J = 8.8 Hz, 2H, Ar*H*), 8.09 (s, 1H, C*H*N). ^{13}C NMR (75 MHz, $CDCl_3$) δ 20.5, 28.7, 43.7, 47.5, 62.1, 114.6, 120.5, 126.3, 126.5, 126.6, 128.9, 129.4, 130.1, 130.9, 131.2, 132.9, 137.1, 139.9, 146.1, 155.9. HRMS-TOF: m/z $[M+H]^+$ 461.1646 (Calcd for $C_{25}H_{25}N_4O_3S$: 461.1653).

4.6.6. 1-(2-((1-(4-((3,4-Dihydroisoquinolin-2(1H)-yl)sulfonyl)phenyl)-1H-1,2,3-triazol-4-yl)methoxy)phenyl)ethanone (**19**)

White solid. 78%. mp 185–186 °C. IR (UATR) cm^{-1}: 1655, 1595, 1450, 1358, 1161. ^1H NMR (300 MHz, $CDCl_3$) δ 2.58 (s, 3H, COCH_3), 2.91 (t, J = 6.0 Hz, 2H, C4–*H*), 3.42 (t, J = 6.0 Hz, 2H, C3–*H*), 4.31 (s, 2H, C1–*H*), 5.38 (s, 2H, CH_2O), 6.99–7.15 (m, 6H, Ar*H*), 7.46 (dt, J = 7.7, 1.7 Hz, 1H, Ar*H*), 7.69 (dd, J = 7.7, 1.7 Hz, 1H, Ar*H*), 7.92 (d, J = 8.8 Hz, 2H, Ar*H*), 7.99 (d, J = 8.8 Hz, 2H, Ar*H*), 8.15 (s, 1H, C*H*N). ^{13}C NMR (75 MHz, $CDCl_3$) δ 28.7, 31.7, 43.7, 47.5, 62.4, 113.1, 120.7, 120.8, 121.5, 126.3, 126.5, 127.0, 128.9, 129.0, 129.5, 130.5, 131.2, 132.9, 133.6, 137.2, 139.7, 145.1, 157.0, 199.7. HRMS-TOF: m/z $[M+Na]^+$ 511.1391 (Calcd for $C_{26}H_{24}N_4NaO_4S$: 511.1410).

4.6.7. Methyl 2-((1-(4-((3,4-dihydroisoquinolin-2(1H)-yl)sulfonyl)phenyl)-1H-1,2,3-triazol-4-yl)methoxy)benzoate (**20**)

White solid. 91%. mp 162–163 °C. IR (UATR) cm^{-1}: 1696, 1599, 1453, 1306, 1254, 1160. ^1H NMR (300 MHz, $CDCl_3$) δ 2.92 (t, J = 6.0 Hz, 2H, C4–*H*), 3.43 (t, J = 6.0 Hz, 2H, C3–*H*), 3.88 (s, 3H, CO_2CH_3), 4.32 (s, 2H, C1–*H*), 5.39 (s, 2H, CH_2O), 7.00–7.18 (m, 6H, Ar*H*), 7.48 (dt, J = 7.8, 1.7 Hz, 1H, Ar*H*), 7.82 (dd, J = 7.8, 1.7 Hz, 1H, Ar*H*), 7.93 (d, J = 8.9 Hz, 2H, Ar*H*), 7.99 (d, J = 8.9 Hz, 2H, Ar*H*), 8.31 (s, 1H, C*H*N). ^{13}C NMR (75 MHz, $CDCl_3$) δ 28.7, 43.7, 47.5, 52.0, 63.4, 114.1, 120.6, 121.0, 121.3, 126.3, 126.5, 127.0, 128.9, 129.4, 131.2, 131.8, 132.9, 133.8, 137.0, 139.9, 146.0, 157.8, 166.1. HRMS-TOF: m/z $[M+Na]^+$ 527.1365 (Calcd for $C_{26}H_{24}N_4NaO_5S$: 527.1360).

4.6.8. 4-((1-(4-((3,4-dihydroisoquinolin-2(1H)-yl)sulfonyl)phenyl)-1H-1,2,3-triazol-4-yl)methoxy)benzaldehyde (**21**)

White solid. 81%. mp 189–190 °C. IR (UATR) cm^{-1}: 1686, 1605, 1578, 1500, 1357, 1243, 1160. ^1H NMR (300 MHz, $CDCl_3$) δ 2.92 (t, J = 5.9 Hz, 2H, C4–*H*), 3.43 (t, J = 5.9 Hz, 2H, C3–*H*), 4.32 (s, 2H, C1–*H*), 5.37 (s, 2H, CH_2O), 7.00–7.18 (m, 6H, Ar*H*), 7.84 (d, J = 8.8 Hz, 2H, Ar*H*), 7.92 (d, J = 8.8 Hz, 2H, Ar*H*), 7.99 (d, J = 8.8 Hz, 2H, Ar*H*), 8.14 (s, 1H, C*H*N), 9.88 (s, 3H, C*H*O). ^{13}C NMR (75 MHz, $CDCl_3$) δ 28.7, 43.7, 47.5, 62.0, 115.1, 120.7, 120.9, 126.3, 126.5, 127.0, 128.9, 129.5, 130.6, 131.2, 132.2, 132.8, 137.4, 139.7, 144.8, 162.9, 190.7. HRMS-TOF: m/z $[M+H]^+$ 475.1450 (Calcd for $C_{25}H_{23}N_4O_4S$: 475.1446).

4.6.9. 4-((1-(4-((3,4-Dihydroisoquinolin-2(1H)-yl)sulfonyl)phenyl)-1H-1,2,3-triazol-4-yl)methoxy)-2H-chromen-2-one (**22**)

White solid. 94%. mp 150–151 °C. IR (UATR) cm^{-1}: 1687, 1618, 1456, 1354, 1248, 1161. ^1H NMR (300 MHz, $CDCl_3$) δ 2.96 (t, J = 5.9 Hz, 2H, C4–*H*), 3.47 (t, J = 5.9 Hz, 2H, C3–*H*), 4.36 (s, 2H, C1–*H*), 5.46 (s, 2H, CH_2O), 5.92 (s, 1H, C*H*CO), 7.04–7.36 (m, 6H, Ar*H*), 7.57 (dt, J = 7.7, 1.4 Hz, 1H, Ar*H*), 7.82 (dd, J = 7.9, 1.4 Hz, 1H, Ar*H*), 7.99 (d, J = 8.7 Hz, 2H, Ar*H*), 8.05 (d, J = 8.7 Hz, 2H, Ar*H*), 8.27 (s, 1H, C*H*N). ^{13}C NMR (75 MHz, $CDCl_3$) δ 28.7, 43.7, 47.5, 62.4, 91.4, 115.4, 116.8, 120.8, 121.5, 123.1, 124.0, 126.3, 126.6, 127.0, 128.9, 129.5, 131.2, 132.7, 132.8, 139.6, 142.9, 153.4, 162.4, 164.8. HRMS-TOF: m/z $[M+H]^+$ 515.1384 (Calcd for $C_{27}H_{23}N_4O_5S$: 515.1384).

*4.6.10. (1-(4-((6,7-Dimethoxy-3,4-dihydroisoquinolin-2(1H)-yl) sulfonyl)phenyl)-1H-1,2,3-triazol-4-yl)methanol (**23**)*

Pale yellow solid. 58%. mp 159–160 °C. IR (UATR) cm^{-1}: 3280, 1599, 1523, 1342, 1226, 1158. ^1H NMR (300 MHz, DMSO-d_6) δ 2.78 (t, J = 5.5 Hz, 2H, C4–*H*), 3.33 (t, J = 5.8 Hz, 2H, C3–*H*), 3.67, 3.68 (2s, 6H, 2 × OC*H*$_3$), 4.16 (s, 2H, C1–*H*), 4.62 (d, J = 5.5 Hz, 2H, C*H*$_2$OH), 5.41 (t, J = 5.4 Hz, 1H, CH$_2$O*H*), 6.67 (s, 1H, Ar*H*), 6.76 (s, 1H, Ar*H*), 7.99 (d, J = 8.8 Hz, 2H, Ar*H*), 8.19 (d, J = 8.8 Hz, 2H, Ar*H*), 8.83 (s, 1H, C*H*N). ^{13}C NMR (75 MHz, DMSO-d_6) δ 28.0, 44.1, 47.4, 55.4, 55.9, 56.0, 110.3, 112.3, 120.8, 121.7, 123.6, 125.2, 129.8, 136.0, 140.2, 147.8, 148.1, 150.1. HRMS-TOF: m/z $[M+H]^+$ 431.1389 (Calcd for $C_{20}H_{23}N_4O_5S$: 431.1384).

*4.6.11. 6,7-Dimethoxy-2-((4-(4-(phenoxymethyl)-1H-1,2,3-triazol-1-yl)phenyl)sulfonyl)-1,2,3,4-tetrahydroisoquinoline (**24**)*

White solid. 91%. mp 158–159 °C. IR (UATR) cm^{-1}: 1597, 1519, 1348, 1227, 1163. ^1H NMR (300 MHz, $CDCl_3$) δ 2.82 (t, J = 6.0 Hz, 2H, C4–*H*), 3.40 (t, J = 6.0 Hz, 2H, C3–*H*), 3.80 (s, 6H, 2 × OC*H*$_3$), 4.24 (s, 2H, C1–*H*), 5.29 (s, 2H, C*H*$_2$O), 6.49 (s, 1H, Ar*H*), 6.53 (s, 1H, Ar*H*), 6.94–7.02 (m, 3H, Ar*H*), 7.24–7.34 (m, 2H, Ar*H*), 7.91 (d, J = 8.8 Hz, 2H, Ar*H*), 7.98 (d, J = 8.8 Hz, 2H, Ar*H*), 8.10 (s, 1H, C*H*N). ^{13}C NMR (75 MHz, $CDCl_3$) δ 28.2, 43.8, 47.2, 55.9, 56.0, 61.9, 109.0, 111.4, 114.7, 120.6, 121.6, 123.0, 124.8, 129.4, 129.7, 137.2, 139.8, 145.9, 147.9, 148.1, 158.0. HRMS-TOF: m/z $[M+H]^+$ 507.1706 (Calcd for $C_{26}H_{27}N_4O_5S$: 507.1697).

*4.6.12. 6,7-Dimethoxy-2-((4-(4-((naphthalen-2-yloxy)methyl)-1H-1,2,3-triazol-1-yl)phenyl)sulfonyl)-1,2,3,4-tetrahydroisoquinoline (**25**)*

Pale yellow solid. 83%. mp 210–211 °C. IR (UATR) cm^{-1}: 1598, 1519, 1463, 1347, 1257, 1163. ^1H NMR (300 MHz, $CDCl_3$) δ 2.86 (t, J = 5.7 Hz, 2H, C4–*H*), 3.43 (t, J = 5.7 Hz, 2H, C3–*H*), 3.83, 3.84 (2s, 6H, 2 × OC*H*$_3$), 4.27 (s, 2H, C1–*H*), 5.45 (s, 2H, C*H*$_2$O), 6.53 (s, 1H, Ar*H*), 6.56 (s, 1H, Ar*H*), 7.22 (dd, J = 8.9, 2.5 Hz, 1H, Ar*H*), 7.31 (d, J = 2.4 Hz, 1H, Ar*H*), 7.38 (t, J = 8.1 Hz, 1H, Ar*H*), 7.47 (t, J = 8.1 Hz, 1H, Ar*H*), 7.75–7.82 (m, 3H, Ar*H*), 7.95 (d, J = 8.9 Hz, 2H, Ar*H*), 8.01 (d, J = 8.9 Hz, 2H, Ar*H*), 8.17 (s, 1H, C*H*N). ^{13}C NMR (75 MHz, $CDCl_3$) δ 28.2, 43.8, 47.2, 55.9, 56.0, 61.9, 107.3, 108.9, 111.4, 118.6, 120.6, 120.7, 123.0, 124.1, 124.8, 126.6, 126.9, 127.7, 129.3, 129.4, 129.7, 134.4, 137.2, 139.8, 145.8, 147.9, 148.1, 155.9. HRMS-TOF: m/z $[M+H]^+$ 557.1843 (Calcd for $C_{30}H_{29}N_4O_5S$: 557.1853).

*4.6.13. 6,7-Dimethoxy-2-((4-(4-((o-tolyloxy)methyl)-1H-1,2,3-triazol-1-yl)phenyl)sulfonyl)-1,2,3,4-tetrahydroisoquinoline (**26**)*

White solid. 87%. mp 138–139 °C. IR (UATR) cm^{-1}: 1596, 1519, 1463, 1346, 1237, 1160. ^1H NMR (300 MHz, $CDCl_3$) δ 2.28 (s, 3H, C*H*$_3$), 2.86 (t, J = 5.9 Hz, 2H, C4–*H*), 3.44 (t, J = 5.9 Hz, 2H, C3–*H*), 3.84 (s, 6H, 2 × OC*H*$_3$), 4.28 (s, 2H, C1–*H*), 5.34 (s, 2H, C*H*$_2$O), 6.53 (s, 1H, Ar*H*), 6.57 (s, 1H, Ar*H*), 6.90–7.02 (m, 2H, Ar*H*), 7.16–7.23 (m, 2H, Ar*H*), 7.96 (d, J = 8.9 Hz, 2H, Ar*H*), 8.02 (d, J = 8.9 Hz, 2H, Ar*H*), 8.11 (s, 1H, C*H*N). ^{13}C NMR (75 MHz, $CDCl_3$) δ 16.3, 28.2, 43.8, 47.2, 55.9, 56.0, 62.1, 109.0, 111.5, 120.6, 121.3, 123.0, 124.2, 124.8, 127.0, 129.4, 129.5, 131.0, 137.2, 139.9, 146.3, 147.9, 148.1, 156.2. HRMS-TOF: m/z $[M+H]^+$ 521.1859 (Calcd for $C_{27}H_{29}N_4O_5S$: 521.1853).

*4.6.14. 6,7-Dimethoxy-2-((4-(4-((p-tolyloxy)methyl)-1H-1,2,3-triazol-1-yl)phenyl)sulfonyl)-1,2,3,4-tetrahydroisoquinoline (**27**)*

White solid. 92%. mp 168–169 °C. IR (UATR) cm^{-1}: 1596, 1509, 1464, 1346, 1225, 1162. ^1H NMR (300 MHz, $CDCl_3$) δ 2.31 (s, 3H, C*H*$_3$), 2.86 (t, J = 5.7 Hz, 2H, C4–*H*), 3.44 (t, J = 5.7 Hz, 2H, C3–*H*), 3.84 (s, 6H, 2 × OC*H*$_3$), 4.28 (s, 2H, C1–*H*), 5.30 (s, 2H, C*H*$_2$O), 6.53 (s, 1H, Ar*H*), 6.56 (s, 1H, Ar*H*), 6.92 (d, J = 8.5 Hz, 2H, Ar*H*), 7.12 (d, J = 8.5 Hz, 2H, Ar*H*), 7.94 (d, J = 8.7 Hz, 2H, Ar*H*), 8.01 (d, J = 8.7 Hz, 2H, Ar*H*), 8.13 (s, 1H, C*H*N). ^{13}C NMR (75 MHz, $CDCl_3$) δ 20.5, 28.2, 43.8, 47.2, 55.9, 56.0, 62.0, 109.0, 111.4, 114.6, 120.6, 123.0, 129.4, 130.1, 130.9, 137.2, 139.9, 146.1, 147.9, 148.1, 155.9. HRMS-TOF: m/z $[M+H]^+$ 521.1842 (Calcd for $C_{27}H_{29}N_4O_5S$: 521.1853).

*4.6.15. 1-(2-((1-(4-((6,7-Dimethoxy-3,4-dihydroisoquinolin-2(1H)-yl)sulfonyl)phenyl)-1H-1,2,3-triazol-4-yl)methoxy)phenyl)ethanone (**28**)*

White solid. 70%. mp 171–172 °C. IR (UATR) cm^{-1}: 1670, 1596, 1519, 1450, 1347, 1226, 1161. ^1H NMR (300 MHz, $CDCl_3$) δ 2.58 (s, 3H, COC*H*$_3$), 2.81 (t, J = 5.7 Hz, 2H, C4–*H*), 3.39 (t, J = 5.7 Hz, 2H, C3–*H*), 3.79, 3.80 (2s, 6H, 2 × OC*H*$_3$), 4.23 (s, 2H, C1–*H*), 5.38 (s, 2H, C*H*$_2$O), 6.49 (s, 1H, Ar*H*), 6.52 (s, 1H, Ar*H*), 7.03 (t, J = 8.0 Hz, 1H, Ar*H*), 7.12 (d, J = 8.2 Hz, 1H, Ar*H*), 7.46 (dt, J = 8.2, 1.8 Hz, 1H, Ar*H*), 7.69 (dd, J = 7.7, 1.8 Hz, 1H, Ar*H*), 7.91 (d, J = 8.9 Hz, 2H, Ar*H*), 7.98 (d, J = 8.9 Hz, 2H, Ar*H*), 8.15 (s, 1H, C*H*N). ^{13}C NMR (75 MHz, $CDCl_3$) δ 28.3, 31.7, 43.8, 47.2, 55.9, 56.0, 62.4, 108.9, 111.4, 113.1, 120.7, 120.8, 121.5, 122.9, 124.8, 129.0, 129.5, 130.5, 133.6, 137.3, 139.7, 145.1, 147.9, 148.1, 157.0, 199.7. HRMS-TOF: m/z $[M+Na]^+$ 571.1608 (Calcd for $C_{28}H_{28}N_4NaO_6S$: 571.1622).

*4.6.16. Methyl 2-((1-(4-((6,7-dimethoxy-3,4-dihydroisoquinolin-2(1H)-yl)sulfonyl)phenyl)-1H-1,2,3-triazol-4-yl)methoxy)benzoate (**29**)*

White solid. 94%. mp 142–143 °C. IR (UATR) cm^{-1}: 1723, 1598, 1519, 1451, 1347, 1258, 1162. ^1H NMR (300 MHz, $CDCl_3$) δ 2.83 (t, J = 5.8 Hz, 2H, C4–*H*), 3.40 (t, J = 5.8 Hz, 2H, C3–*H*), 3.80 (s, 6H, 2 × OC*H*$_3$), 3.87 (s, 3H, CO$_2$C*H*$_3$), 4.24 (s, 2H, C1–*H*), 5.38 (s, 2H, C*H*$_2$O), 6.50 (s, 1H, Ar*H*), 6.53 (s, 1H, Ar*H*), 7.02 (t, J = 8.2 Hz, 1H, Ar*H*), 7.12 (d, J = 8.3 Hz, 1H, Ar*H*), 7.48 (dt, J = 8.2, 1.8 Hz, 1H, Ar*H*), 7.82 (dd, J = 7.8, 1.7 Hz, 1H, Ar*H*), 7.94 (d, J = 8.9 Hz, 2H, Ar*H*), 7.99 (d, J = 8.9 Hz, 2H, Ar*H*), 8.31 (s, 1H, C*H*N). ^{13}C NMR (75 MHz, $CDCl_3$) δ 28.3, 43.8, 47.2, 52.0, 55.9, 56.0, 63.4, 108.9, 111.4, 114.0, 120.5, 120.6, 121.0, 121.3, 123.0, 124.8, 129.4, 131.9, 133.8, 137.0, 139.9, 146.0, 147.8, 148.0, 157.8, 166.1. HRMS-TOF: m/z $[M+H]^+$ 565.1737 (Calcd for $C_{28}H_{29}N_4O_7S$: 565.1752).

*4.6.17. 4-((1-(4-((6,7-Dimethoxy-3,4-dihydroisoquinolin-2(1H)-yl) sulfonyl)phenyl)-1H-1,2,3-triazol-4-yl)methoxy)benzaldehyde (**30**)*

White solid. 80%. mp 186–187 °C. IR (UATR) cm^{-1}: 1692, 1604, 1519, 1348, 1231, 1162. ^1H NMR (300 MHz, $CDCl_3$) δ 2.86 (t, J = 5.8 Hz, 2H, C4–*H*), 3.45 (t, J = 5.8 Hz, 2H, C3–*H*), 3.84 (s, 6H, 2 × OC*H*$_3$), 4.29 (s, 2H, C1–*H*), 5.42 (s, 2H, C*H*$_2$O), 6.53 (s, 1H, Ar*H*), 6.56 (s, 1H, Ar*H*), 7.15 (d, J = 8.7 Hz, 2H, Ar*H*), 7.88 (d, J = 8.7 Hz, 2H, Ar*H*), 7.95 (d, J = 8.8 Hz, 2H, Ar*H*), 8.04 (d, J = 8.8 Hz, 2H, Ar*H*), 8.17 (s, 1H, C*H*N), 9.92 (s, 1H, C*H*O). ^{13}C NMR (75 MHz, $CDCl_3$) δ 28.2, 43.8, 47.2, 55.9, 56.0, 62.0, 109.0, 111.5, 115.1, 120.6, 120.9, 123.0, 124.8, 129.5, 130.6, 132.1, 137.5, 139.7, 144.8, 147.9, 148.1, 162.9, 190.6. HRMS-TOF: m/z $[M+H]^+$ 535.1645 (Calcd for $C_{27}H_{27}N_4O_6S$: 535.1646).

*4.6.18. 6,7-Dimethoxy-2-((4-(4-((4-nitrophenoxy)methyl)-1H-1,2,3-triazol-1-yl)phenyl)sulfonyl)-1,2,3,4-tetrahydroisoquinoline (**31**)*

White solid. 77%. mp 173–174 °C. IR (UATR) cm^{-1}: 1592, 1518, 1464, 1341, 1257, 1162. ^1H NMR (300 MHz, $CDCl_3$) δ 2.86 (t, J = 5.9 Hz, 2H, C4–*H*), 3.45 (t, J = 5.9 Hz, 2H, C3–*H*), 3.84 (s, 6H, 2 × OC*H*$_3$), 4.29 (s, 2H, C1–*H*), 5.42 (s, 2H, C*H*$_2$O), 6.53 (s, 1H, Ar*H*), 6.56 (s, 1H, Ar*H*), 7.12 (d, J = 7.3 Hz, 2H, Ar*H*), 7.96 (d, J = 8.8 Hz, 2H, Ar*H*), 8.03 (d, J = 8.8 Hz, 2H, Ar*H*), 8.19 (s, 1H, C*H*N), 8.25 (d, J = 7.3 Hz, 2H, Ar*H*). ^{13}C NMR (75 MHz, $CDCl_3$) δ 28.2, 43.8, 47.2, 55.9, 56.0, 62.3, 108.9, 111.4, 114.8, 120.7, 121.0, 122.9, 124.8, 126.0, 129.5, 137.5, 139.5, 142.1, 144.3, 148.1, 162.8. HRMS-TOF: m/z $[M+H]^+$ 552.1539 (Calcd for $C_{26}H_{26}N_5O_7S$: 552.1548).

*4.6.19. 3-((1-(4-((6,7-dimethoxy-3,4-dihydroisoquinolin-2(1H)-yl) sulfonyl)phenyl)-1H-1,2,3-triazol-4-yl)methoxy)-4-methoxybenzaldehyde (**32**)*

Pale yellow solid. 76%. mp 141–142 °C. IR (UATR) cm^{-1}: 1682, 1587, 1519, 1464, 1346, 1260, 1161. ^1H NMR (300 MHz, $CDCl_3$) δ 2.86 (t, J = 5.8 Hz, 2H, C4–*H*), 3.44 (t, J = 5.8 Hz, 2H, C3–*H*), 3.83, 3.84, 3.95 (3s, 9H, 3 × O*CH*$_3$), 4.27 (s, 2H, C1–*H*), 5.48 (s, 2H, *CH*$_2$O), 6.53 (s, 1H, Ar*H*), 6.56 (s, 1H, Ar*H*), 7.24 (d, J = 7.9 Hz, 1H, Ar*H*), 7.46 (s, 1H, Ar*H*), 7.47 (d, J = 8.0 Hz, 1H, Ar*H*), 7.94 (d, J = 8.8 Hz, 2H, Ar*H*), 8.01 (d, J = 8.8 Hz, 2H, Ar*H*), 8.21 (s, 1H, C*H*N), 9.88 (s, 1H, C*H*O). ^{13}C NMR (75 MHz, $CDCl_3$) δ 28.2, 43.8, 47.2, 55.9, 56.0, 62.7, 109.0, 109.5, 111.5, 112.6, 120.6, 121.2, 123.0, 124.8, 126.6, 129.4, 130.9, 137.4, 139.7, 144.8, 147.9, 148.1, 150.0, 152.8, 190.8. HRMS-TOF: m/z $[M+H]^+$ 565.1759 (Calcd for $C_{28}H_{29}N_4O_7S$: 565.1752).

*4.6.20. 4-((1-(4-((6,7-Dimethoxy-3,4-dihydroisoquinolin-2(1H)-yl) sulfonyl)phenyl)-1H-1,2,3-triazol-4-yl)methoxy)-3-methoxybenzaldehyde (**33**)*

Pale yellow solid. 77%. mp 116–117 °C. IR (UATR) cm^{-1}: 1683, 1596, 1518, 1437, 1346, 1264, 1162. ^1H NMR (300 MHz, $CDCl_3$) δ 2.87 (t, J = 5.7 Hz, 2H, C4–*H*), 3.46 (t, J = 5.9 Hz, 2H, C3–*H*), 3.84, 3.99 (2s, 9H, 3 × O*CH*$_3$), 4.28 (s, 2H, C1–*H*), 5.44 (s, 2H, *CH*$_2$O), 6.54 (s, 1H, Ar*H*), 6.57 (s, 1H, Ar*H*), 7.04 (d, J = 8.3 Hz, 1H, Ar*H*), 7.55 (dd, J = 8.2, 1.8 Hz, 1H, Ar*H*), 7.61 (d, J = 1.8 Hz, 1H, Ar*H*), 7.95 (d, J = 8.8 Hz, 2H, Ar*H*), 8.02 (d, J = 8.8 Hz, 2H, Ar*H*), 8.20 (s, 1H, C*H*N), 9.88 (s, 1H, C*H*O). ^{13}C NMR (75 MHz, $CDCl_3$) δ 28.2, 43.8, 47.2, 56.0, 56.2, 62.8, 108.9, 111.1, 111.4, 112.0, 120.7, 121.0, 123.0, 124.8, 127.2, 129.4, 130.1, 137.3, 139.8, 144.9, 148.1, 155.0, 190.6. HRMS-TOF: m/z $[M+H]^+$ 565.1753 (Calcd for $C_{28}H_{29}N_4O_7S$: 565.1752).

4.7. Cytotoxic assay: cancer cell lines

Cell lines suspended in the corresponding culture medium were inoculated in 96-well microtiter plates (Corning Inc., NY, USA) at a density of 10,000–20,000 cells per well and incubated at 37 °C in a humidified atmosphere with 95% air and 5% CO_2. After 24 h, an equal volume of additional medium containing either the serial dilutions of the test compounds, positive control (etoposide and/or doxorubicin) or negative control (DMSO) was added to the desired final concentrations, and the microtiter plates were further incubated for an additional 48 h. The number of surviving cells in each well was determined using either MTT assay [32,33] (for adherent cells: HuCCA-1, HepG2, and A549 cells) or XTT assay [34] (for suspended cells: MOLT-3 cells) in order to determine the IC_{50}, which is defined as the concentration that inhibits cell growth by 50% (relative to negative control) after 48 h of continuous exposure to each test compound.

4.8. Cytotoxicity assay: primate cell line (Vero)

The cytotoxicity was performed by using the Green Fluorescent Protein (GFP) detection method [35]. The GFP-expressing Vero cell line was generated in-house by stably transfecting the African green monkey kidney cell line (Vero, ATCC CCL-81), with pEGFP-N1 plasmid (Clontech). The cell line was maintained in a minimal essential medium supplemented with 10% heat-inactivated fetal bovine serum, 2 mM L-glutamine, 1 mM sodium pyruvate, 1.5 g/L sodium bicarbonate and 0.8 mg/mL geneticin, at 37 °C in a humidified incubator with 5% CO_2. The assay was carried out by adding 45 μL of cell suspension at 3.3×10^4 cells/mL to each well of 384-well plates containing 5 μL of test compounds previously diluted in 0.5% DMSO, and then incubating for 4 days in 37 °C incubator with 5% CO_2. Fluorescence signals were measured by using SpectraMax M5 microplate reader (Molecular Devices, USA) in the bottom reading mode with excitation and emission wavelengths of 485 and 535 nm. Fluorescence signal at day 4 was subtracted with background fluorescence at day 0. IC_{50} values were derived from dose–response curves, using 6 concentrations of 3-fold serially diluted samples, by the SOFTMax Pro software (Molecular device). Ellipticine and 0.5% DMSO were used as a positive and a negative control, respectively.

4.9. Identification of putative targets of 1,2,3,4-tetrahydroisoquinolines

A structure similarity search was performed in PubChem using compounds **20** and **27** as the query molecules, which identified 1-[4-(3,4-dihydro-1*H*-isoquinolin-2-ylsulfonyl)phenyl]pyrrolidin-2-one **7** (CID 18096680) as homologous structure. Analysis on the previously tested bioactivity of this compound revealed 17β-hydroxysteroid dehydrogenase type 5, belonging to the aldo-keto reductase family 1 member C3 (AKR1C3), as a putative target affording potent nanomolar inhibitory activity with IC_{50} values of 42 and 52 nM as verified by two separate bioactivity experiments [11,12]. In addition, the X-ray crystallographic structure of AKR1C3 as obtained from the Protein Data Bank (PDB id 4FAL) was co-complexed with 3-(3,4-dihydroisoquinolin-2(1*H*)-ylsulfonyl)-*N*-methylbenzamide (**8**), which displayed 2-(benzenesulfonyl)-1,2,3,4-tetrahydroisoquinoline as a similar moiety to compounds investigated herein.

4.10. Molecular docking

Molecular docking was performed as to shed light on the binding modalities of investigated ligands toward its putative target AKR1C3 using a similar protocol as previously described [36]. Preparation of the AKR1C3 protein structure prior to docking was performed by adding essential hydrogen atoms using Kollman united atom charges and solvation parameters as provided by AutoDock Tools in PyRx 0.6 [37]. 1,2,3,4-Tetrahydroisoquinoline-triazole structures were constructed using Marvin Sketch Version 6.0 [38] and geometrically optimized with Gaussian 09 [39] using the B3LYP/6-31G(d) method. Ligand structures were prepared for docking by merging non-polar hydrogen atoms, adding Gasteiger partial charges and defining rotatable bonds. A maximum grid box size of 47.27 × 49.52 × 59.94 Å was generated to cover the entire AKR1C3 protein using Auto Grid. The grid box was allocated at the center of the protein using *x,y,z* coordinates of 7.1616, 5.6316, 11.0790, respectively. Molecular docking simulations were performed using AutoDock Vina as part of the PyRx 0.6 software. The co-crystallized ligand was re-docked as validation of the docking protocol. Docked structures were visualized using PyMOL [40]. A 2-dimensional schematic representation of protein-ligand interaction was generated using PoseViewWeb version 1.97.0 [41].

Acknowledgments

This project was financially supported from Srinakharinwirot University under the Government Budget (B.E. 2558) and the Thailand Research Fund under the Young Scholars Research Fellowship (MRG5680001 to R.P.). Great supports from the Office of Higher Education Commission and Mahidol University under the National Research Universities Initiative are appreciated. We are also indebted to Chulabhorn Research Institute for recording mass spectra and bioactivity testing.

Appendix A. Supplementary data

Supplementary data related to this article can be found at http://dx.doi.org/10.1016/j.ejmech.2014.05.019.

References

[1] K.W. Bentley, in: The Isoquinoline Alkaloids, Harwood Academic Publishers, Amsterdam, 1998.
[2] J.D. Scott, R.M. Williams, Chemistry and biology of the tetrahydroisoquinoline antitumor antibiotics, Chem. Rev. 102 (2002) 1669–1730.
[3] P. Siengalewicz, U. Rinner, J. Mulzer, Recent progress in the total synthesis of naphthyridnomycin and lemonomycin tetrahydroisoquinoline antibiotics (TAAs), Chem. Soc. Rev. 37 (2008) 2676–2690.
[4] E.D. Cox, J.M. Cook, The Pictet-Spengler condensation: a new direction for an old reaction, Chem. Rev. 95 (1995) 1797–1842.
[5] E.L. Larghi, M. Amongero, A.B.J. Bracca, T.S. Kaufman, The intermolecular Pictet-Spengler condensation with chiral carbonyl derivatives in the stereoselective syntheses of optically active isoquinoline and indole alkaloids, ARKIVOC 12 (2005) 98–153.
[6] R. Pingaew, A. Worachartcheewan, C. Nantasenamat, S. Prachayasittikul, S. Ruchirawat, V. Prachayasittikul, Synthesis, cytotoxicity and QSAR study of *N*-tosyl-1,2,3,4-tetrahydroisoquinoline derivatives, Arch. Pharm. Res. 36 (2013) 1066–1077.
[7] R. Pingaew, S. Prachayasittikul, S. Ruchirawat, V. Prachayasittikul, Synthesis and cytotoxicity of novel *N*-sulfonyl-1,2,3,4-tetrahydroisoquinoline thiosemicarbazone derivatives, Med. Chem. Res. 22 (2013) 267–277.
[8] R. Gitto, S. Agnello, S. Ferro, L. De Luca, D. Vullo, J. Brynda, P. Mader, C.T. Supuran, A. Chimirri, Identification of 3,4-dihydroisoquinoline-2(1*H*)-sulfonamide as potent carbonic anhydrase inhibitors: synthesis, biological evaluation, and enzyme–ligand X-ray studies, J. Med. Chem. 53 (2010) 2401–2408.
[9] D. Ma, W. Wu, G. Yang, J. Li, J. Li, Q. Ye, Tetrahydroisoquinoline based sulfonamide hydroxamates as potent matrix metalloproteinase inhibitors, Bioorg. Med. Chem. Lett. 14 (2004) 47–50.
[10] H. Matter, M. Schudok, W. Schwab, W. Thorwart, D. Barbier, G. Billen, B. Haase, B. Neises, K. Weithmann, T. Wollmann, Tetrahydroisoquinoline-3-carboxylate based matrix-metalloproteinase inhibitors: design, synthesis and structure–activity relationship, Bioorg. Med. Chem. 10 (2002) 3529–3544.
[11] S.M.F. Jamieson, D.G. Brooke, D. Heinrich, G.J. Atwell, S. Silva, E.J. Hamilton, A.P. Turnbull, L.J.M. Rigoreau, E. Trivier, C. Soudy, S.S. Samlal, P.J. Owen, E. Schroeder, T. Raynham, J.U. Flanagan, W.A.J. Denny, 3-(3,4-Dihydroisoquinolin-2(1*H*)-ylsulfonyl)benzoic Acids: highly potent and selective inhibitors of the type 5 17-β-hydroxysteroid dehydrogenase AKR1C3, J. Med. Chem. 55 (2012) 7746–7758.
[12] D.M. Heinrich, J.U. Flanagan, S.M.F. Jamieson, S. Silva, L.J.M. Rigoreau, E. Trivier, T. Raynham, A.P. Turnbull, W.A. Denny, Synthesis and structure-activity relationships for 1-(4-(piperidin-1-ylsulfonyl)phenyl)pyrrolidin-2-ones as novel non-carboxylate inhibitors of the aldo-keto reductase enzyme AKR1C3, Eur. J. Med. Chem. 62 (2013) 738–744.
[13] O.A. Barski, S.M. Tipparaju, A. Bhatnagar, The aldo-keto reductase superfamily and its role in drug metabolism and detoxification, Drug Metab. Rev. 40 (2008) 553–624.
[14] T.M. Penning, M.E. Burczynski, J.M. Jez, C.F. Hung, H.K. Lin, H. Ma, M. Moore, N. Palackal, K. Ratnam, Human 3α-hydroxysteroid dehydrogenase isoforms (AKR1C1-AKR1C4) of the aldo-keto reductase superfamily: functional plasticity and tissue distribution reveals roles in the inactivation and formation of male and female sex hormones, Biochem. J. 351 (2000) 67–77.
[15] M.C. Byrns, Y. Jin, T.M. Penning, Inhibitors of type 5 17β-hydroxysteroid dehydrogenase (AKR1C3): overview and structural insights, J. Steroid Biochem. Mol. Biol. 125 (2011) 95–104.
[16] J.U. Flanagan, Y. Yosaatmadja, R.M. Teague, M.Z.L. Chai, A.P. Turnbull, C.J. Squire, Crystal structures of three classes of non-steroidal anti-inflammatory drugs in complex with aldo-keto reductase 1C3, PLoS One 7 (2012) e43965.
[17] S.G. Agalave, S.R. Maujan, V.S. Pore, Click chemistry: 1,2,3-triazoles as pharmacophores, Chem. Asian J. 6 (2011) 2696–2718.
[18] X. Li, Y. Lin, Y. Yuan, K. Liu, X. Qian, Novel efficient anticancer agents and DNA-intercalators of 1,2,3-triazol-1,8-naphthalimides: design, synthesis, and biological activity, Tetrahedron 67 (2011) 2299–2304.
[19] X.L. Wang, K. Wan, C.H. Zhou, Synthesis of novel sulfanilamide-derived 1,2,3-triazoles and their evaluation for antibacterial and antifungal activities, Eur. J. Med. Chem. 45 (2010) 4631–4639.
[20] R. Pingaew, S. Prachayasittikul, S. Ruchirawat, V. Prachayasittikul, Synthesis and cytotoxicity of novel 4-(4-(substituted)-1*H*-1,2,3-triazol-1-yl)-*N*-phenethylbenzenesulfonamides, Med. Chem. Res. 23 (2014) 1768–1780.
[21] S.P. Miller, Y.L. Zhong, Z. Liu, M. Simeone, N. Yasuda, J. Limanto, Z. Chen, J. Lynch, V. Capodanno, Practical and cost-effective manufacturing route for the synthesis of a β-lactamase inhibitor, Org. Lett. 16 (2014) 174–177.
[22] R. Pingaew, S. Prachayasittikul, S. Ruchirawat, V. Prachayasittikul, Tungstophosphoric acid catalyzed synthesis of *N*-sulfonyl-1,2,3,4-tetrahydroisoquinoline analogs, Chin. Chem. Lett. 24 (2013) 941–944.
[23] R.J. Pagliero, R. Mercado, V. McCracken, M.R. Mazzieri, M.J. Nieto, Rapid and facile synthesis of *N*-benzenesulfonyl derivatives of heterocycles and their antimicrobial properties, Lett. Drug Des. Discov. 8 (2011) 778–791.
[24] E.M. Guantai, K. Ncokazi, T.J. Egan, J. Gut, P.J. Rosenthal, P.J. Smith, K. Chibale, Design, synthesis and in vitro antimalarial evaluation of triazole-linked chalcone and dienone hybrid compounds, Bioorg. Med. Chem. 18 (2010) 8243–8256.
[25] Y. Tsuzuki, T.K.N. Nguyen, D.R. Garud, B. Kuberan, M. Koketsu, 4-Deoxy-4-fluoro-xyloside derivatives as inhibitors of glycosaminoglycan biosynthesis, Bioorg. Med. Chem. Lett. 20 (2010) 7269–7273.
[26] T. Achard, A. Lepronier, Y. Gimbert, H. Clavier, L. Giordano, A. Tenaglia, G. Buono, A regio- and diastereoselective platinum-catalyzed tandem [2+1]/[3+2] cycloaddition sequence, Angew. Chem. Int. Ed. 50 (2011) 3552–3556.
[27] C. Efe, I.N. Lykakis, M. Stratakis, Gold nanoparticles supported on TiO_2 catalyse the cycloisomerisation/oxidative dimerisation of aryl propargyl ethers, Chem. Commun. 47 (2011) 803–805.
[28] R.H. Hans, E.M. Guantai, C. Lategan, P.J. Smith, B. Wan, S.G. Franzblau, J. Gut, P.J. Rosenthal, K. Chibale, Synthesis, antimalarial and antitubercular activity of acetylenic chalcones, Bioorg. Med. Chem. Lett. 20 (2010) 942–944.
[29] I.N. Lykakis, C. Efe, C. Gryparis, M. Stratakis, $Ph_3PAuNTf_2$ as a superior catalyst for the selective synthesis of 2*H*-chromenes: application to the concise synthesis of benzopyran natural products, Eur. J. Org. Chem. (2011) 2334–2338.
[30] C.P. Rao, G. Srimannarayana, Claisen rearrangement of 4-propargloxycoumarins: formation of 2*H*,5*H*-Pyrano[3,2-*c*][1]benzopyran-5-ones, Syn. Commun. 20 (1990) 535–540.
[31] S.C. Zammit, A.J. Cox, R.M. Gow, Y. Zhang, D.J. Kelly, S.J. Williamsa, Evaluation and optimization of antifibrotic activity of cinnamoyl anthranilates, Bioorg. Med. Chem. Lett. 19 (2009) 7003–7006.
[32] J. Carmichael, W.G. DeGraff, A.F. Gazdar, J.D. Minna, J.B. Mitchell, Evaluation of a tetrazolium-based semiautomated colorimetrie assay: assessment of radiosensitivity, Cancer Res. 47 (1987) 943–946.
[33] T. Mosmann, Rapid colorimetric assay for cellular growth and survival: application to proliferation and cytotoxicity assays, J. Immunol. Methods 65 (1983) 55–63.
[34] A. Doyle, J.B. Griffiths, Mammalian Cell Culture: Essential Techniques, John Wiley & Sons, Chichester, UK, 1997.
[35] L. Hunt, M. Jordan, M. De Jesus, F.M. Wurm, GFP-expressing mammalian cells for fast, sensitive, noninvasive cell growth assessment in a kinetic mode, Biotechnol. Bioeng. 65 (1999) 201–205.
[36] N. Suvannang, C. Nantasenamat, C. Isarankura-Na-Ayudhya, V. Prachayasittikul, Molecular docking of aromatase inhibitors, Molecules 16 (2011) 3597–3617.
[37] S. Dallakyan, PyRx Version 0.6, 2013. http://pyrx.scripps.edu.
[38] ChemAxon, Marvin Sketch Version 6.0, 2013. Budapest, Hungary.
[39] M.J. Frisch, G.W. Trucks, H.B. Schlegel, G.E. Scuseria, M.A. Robb, J.R. Cheeseman, G. Scalmani, V. Barone, B. Mennucci, G.A. Petersson, H. Nakatsuji, M. Caricato, X. Li, H.P. Hratchian, A.F. Izmaylov, J. Bloino, G. Zheng, J.L. Sonnenberg, M. Hada, M. Ehara, K. Toyota, R. Fukuda, J. Hasegawa, M. Ishida, T. Nakajima, Y. Honda, O. Kitao, H. Nakai, T. Vreven, J.A. Montgomery, J.E. Peralta, F. Ogliaro, M. Bearpark, J.J. Heyd, E. Brothers, K.N. Kudin, V.N. Staroverov, R. Kobayashi, J. Normand, K. Raghavachari, A. Rendell, J.C. Burant, S.S. Iyengar, J. Tomasi, M. Cossi, N. Rega, J.M. Millam, M. Klene, J.E. Knox, J.B. Cross, V. Bakken, C. Adamo, J. Jaramillo, R. Gomperts, R.E. Stratmann, O. Yazyev, A.J. Austin, R. Cammi, C. Pomelli, J.W. Ochterski, R.L. Martin, K. Morokuma, V.G. Zakrzewski, G.A. Voth, P. Salvador, J.J. Dannenberg, S. Dapprich, A.D. Daniels, Farkas, J.B. Foresman, J.V. Ortiz, J. Cioslowski, D.J. Fox, Gaussian 09, 2009. Wallingford, Connecticut.
[40] W. Delano, PyMOL Release 0.99, DeLano Scientific LLC, Palo Alto, CA, 2002.
[41] K. Stierand, M. Rarey, Drawing the PDB: protein-ligand complexes in two dimensions, ACS Med. Chem. Lett. 1 (2010) 540–545.